Photoinduced Electron Transfer and Molecular Orientation of Zinc Porphyrin−Imide Dyads in Langmuir−Blodgett Monolayer Films

Tomoko Yamazaki, Iwao Yamazaki,* and Atsuhiro Osuka†

Department of Molecular Chemistry, Graduate School of Engineering, Hokkaido University, Sapporo 060-8628, Japan, and Department of Chemistry, Graduate School of Science, Kyoto University, Sakyo-ku, Kyoto 606-8224, Japan

Received: May 19, 1998; In Final Form: July 22, 1998

Photoinduced electron transfer has been studied for bridged donor/acceptor compounds incorporated in Langmuir−Blodgett (LB) films of phospholipid matrix, dioleoylphosphatidylcholine (DOPC). The compounds under investigation are zinc porphyrin (ZnP)−pyromellitimide (D1), ZnP−naphthalenetetracarboxamide (D2), and the derivatives of D1 and D2 with long alkyl chains in the ZnP ring periphery (D3 and D4, respectively). The kinetics of intra- or intermolecular electron transfer was investigated by probing fluorescence quenching of photoexcited ZnP* with the picosecond time-resolved fluorescence measurement. A fast intramolecular electron transfer occurs only in D4-LB film similarly to that in solution ($\tau_f = 16$ ps), but not in D1 and D3. In D2-LB film where D2 molecules are distributed as dimer and higher aggregates as well as monomer, an intermolecular electron transfer ($\tau_f = 48$ ps) occurs at dimer sites instead of the intramolecular reaction. To examine the spatial conformation of D2 dimer in LB monolayer films, the polarized absorption spectra were measured, suggesting a slightly slipped head-to-tail dimerization of two ZnP rings in which ZnP rings are tilted (15°) to the substrate plane.

1. Introduction

Recent studies on photoinduced electron transfer have been directed toward fast reaction kinetics in organized molecular systems in which electron donor and acceptor are chemically linked with close proximity.[1−6] Molecules in such systems can be coupled to an adjacent molecule with relatively strong intermolecular interaction in the excited state, and therefore they may undergo fast photoinduced reactions. An example of such ultrafast electron transfer can be seen in biological photosynthetic reaction centers, and the reaction kinetics and mechanism are examined extensively through time-resolved spectroscopies and theoretical models.[1,7,8] In previous studies, many types of macromolecules mimicking the photosynthetic reaction center were synthesized and examined kinetic properties of the intramolecular electron transfer.[2−6] Most of previous works were performed for solution and demonstrated that solvents surrounding a donor−acceptor molecular system affect strongly reaction kinetics through the reorganization energy and exergonicities. Note that the molecular environment inside the proteins of photosynthetic reaction centers is hydrophobic in nature, and there exists almost no solvent molecule around the molecular systems.[7] It is pointed out, however, that a collective electric field due to amino acid residue surrounding the molecular system plays a role in ultrafast electron transfer.[9,10] In this concept, a study of molecular systems in solid matrix without contact interaction with solvents will provide us with basic information on the intramolecular reaction kinetics.

In an effort to examine an intramolecular electron transfer in solid matrices, we have prepared Langmuir−Blodgett (LB) films containing macromolecules consisting of electron donor (D) and acceptor (A) which are linked chemically with close proximity. Here, we are concerned with macromolecules including zinc porphyrin (D) and diimides (A) which were synthesized previously by Osuka et al.[3] and studied the fast reaction kinetics in solutions.[11,12] When porphyrin and its derivatives are incorporated in solid matrices like LB films, a problem arises regarding molecular aggregation. Porphyrins in general exhibit a strong tendency to form dimers, particularly in LB monolayer films composed of conventional fatty acids like stearic acid. In dimers and higher aggregates, an excited state is deactivated rapidly competing with or exceeding the electron transfer reaction. Here, we prepare LB films composed of phospholipid matrix, dioleoylphosphatidylcholine (DOPC), which allows us to deposit a monolayer on a quartz substrate[13] and to minimize formation of dimer and higher aggregates of porphyrin.[14−16]

In the present paper, we will report on (1) the membrane properties of DOPC-LB films incorporating Osuka's macromolecules (section 3.1), (2) the electron transfer kinetics in solid films probed by a picosecond time-resolved fluorescence spectroscopy (section 3.2−3.3), (3) discussion based on theoretical calculation of the free energy change associated with the electron transfer reaction (section 3.4), and (4) as a special case, formation of dimer and higher aggregates of D2 in LB monolayer films, and the dimer conformation and the orientation of D2 in LB film analyzed through a polarized absorption measurement (section 3.5).

2. Experimental Section

In the present study, we are concerned with four kinds of molecular systems which are composed of zinc porphyrin with and without alkyl chains (ZnP and ZnP′, respectively) as electron donor and pyromellitimide (Pm) or 1,8:4,5-naphthalenetetracarboxamide (Nm) as electron acceptor, i.e., ZnP−Pm (hereafter referred to as D1), ZnP−Nm (D2), ZnP′−Pm (D3), and ZnP′−

* Address correspondence to this author. Phone: 81-11-706-6606. Fax: 81-11-709-2037. E-mail: yamiw@eng.hokudai.ac.jp.
† Kyoto University.

S1089-5647(98)02302-5 CCC: $15.00
Published on Web 09/09/1998

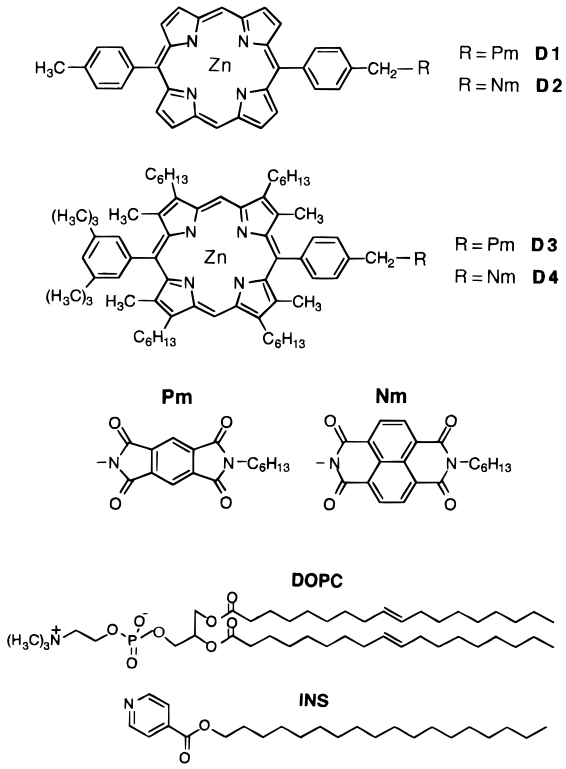

Figure 1. Four kinds of dyads, D1−D4, and matrices for LB monolayer films concerned in the present study. These dyads composed of electron donor (ZnP) and acceptor (Pm or Nm) were incorporated in LB monolayers of DOPC and/or INS.

Nm (D4). The molecular formula are illustrated in Figure 1. The syntheses of these macromolecules are described in previous papers.[11,12] As a matrix of monolayer films, a kind of phospholipid, dioleoylphosphatidylcholine (DOPC, Sigma Chem. Co.), and isonicotinic stearate (INS) were used (see Figure 1). INS was synthesized following a method described in the literature.[17] Monolayer films of DOPC and/or DOPC−INS containing respective molecules were expanded on a surface of water subphase in a trough (San-Yesu SFC-20) at 15 °C. The $\pi-A$ isotherms were measured and then the monolayers were deposited on a quartz plate usually at surface pressure of 20−30 mN.

Polarized absorption spectra were measured with a JASCO U-best 50 spectrophotometer equipped with sheet polarizers having >8% transmittance and >99% polarization in wavelengths above 300 nm. In order to subtract the background in weak absorption spectra, an LB film which is the same as the sample film except that it did not contain the reacting molecules was used as the reference sample. The measurements were performed on the samples of LB films deposited on one side and on both sides of a quartz substrate. The results of analyses were in good agreement between the two types of samples.

The fluorescence decay curves and the time-resolved fluorescence spectra were measured by using a picosecond single-photon timing apparatus. A second harmonics of a Ti:sapphire laser (Coherent MIRA 900) at 410−420 nm was used for the excitation laser pulse. The fluorescence emission was detected with a microchannel-plate photomultiplier (Hamamatsu R3890-U). The instrumental response function obtained from scattered light of a vesicle aqueous solution had a width of 30 ps (fwhm). The fluorescence decay curves and time-resolved spectra were obtained with a method described elsewhere.[18] All the decay measurements of the LB films were carried out in vacuo in order to prevent photobleaching of the sample.

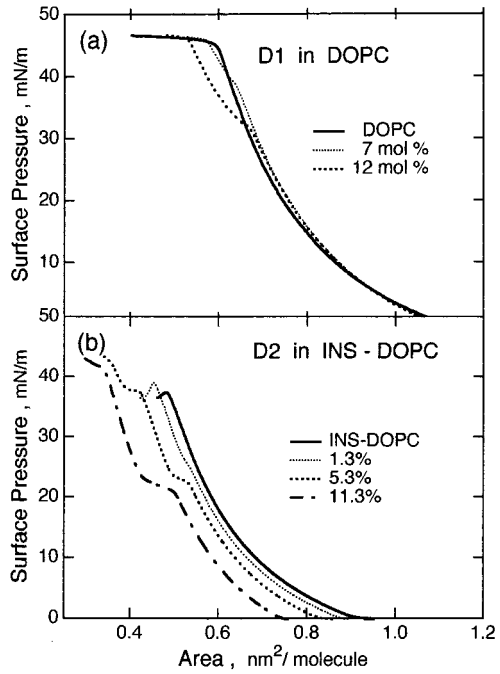

Figure 2. Surface pressure−area isotherms at various concentrations: (a) D1 in DOPC monolayers, and (b) D2 in INS-DOPC (40.5 mol %) mixed monolayers.

3. Results and Discussion

3.1. Preparation of Monolayer Films and Deposition on Quartz Substrates. Figure 2a shows $\pi-A$ curves of DOPC monolayer containing D1, as an example, with different concentrations. It is seen that an expanded liquid phase is formed on a surface of water subphase, and the curves are constant irrespective of concentration of D1 except for higher pressure region above 30 mN/m. Other cases of DOPC-D2, -D3, and -D4 show $\pi-A$ curves almost identical to those of D1 shown in the figure. In the case of D2, however, as is shown in the later discussion, the fluorescence decay data exhibited much larger contribution from dimer and/or higher aggregates in monolayer films than in other cases. Then we used additionally a mixture of DOPC and INS as a matrix of monolayer film. When INS is added to DOPC-D2 membrane, it is expected that molecular aggregation of D2 is restrained because of coordination of a pyridine group of INS onto zinc atom of ZnP in D2. The $\pi-A$ curves of INS-DOPC-D2 monolayers are shown in Figure 2b. The curves shift to lower area side than those of DOPC monolayer, and the surface area was decreased with increasing concentration of D2. These behaviors may be interpreted as arising from a specific spatial arrangement of ZnP in which the ZnP-ring planes are oriented nearly horizontal and parallel to the membrane plane, and the space above the ZnP ring is filled with INS molecule. This model finds strong support from the polarized absorption measurement, as shown in a later discussion (section 3.5). Then an increase of D2 concentration results in much larger number of INS's occupying the space above the ZnP rings. Moreover, it is seen that the monolayer of D2 at higher concentrations exhibits a phase transition at 21−23 mN/m. To examine membrane properties, monolayers of INS-DOPC-D2 were deposited onto a substrate at two surface pressures lower (18−20 mN/m) and higher (30 mN/m) than the phase transition pressure. These two deposited films gave different absorption spectra, and this behavior will be discussed in section 3.5.

All the monolayers of DOPC and INS-DOPC containing D1−D4 allowed us to deposit only a single monolayer, and

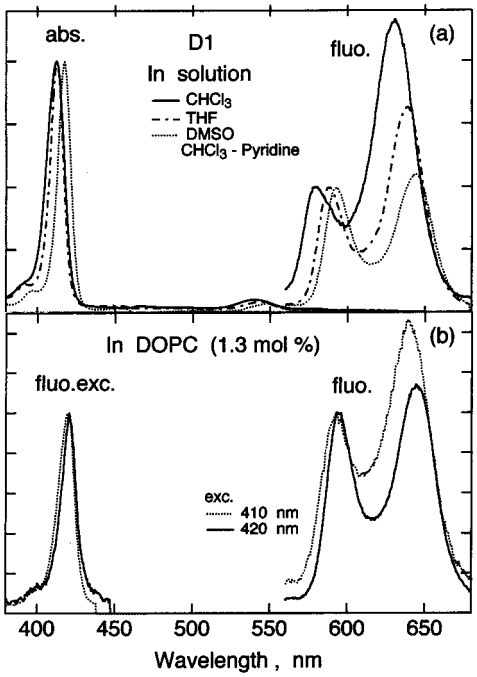

Figure 3. Absorption and steady-state fluorescence spectra of D1 in solution (a) and in LB monolayer film (b). The spectrum in $CHCl_3$−pyridine solution was the same as that in DMSO. The absorption spectra of LB films are shown in the fluorescence excitation spectra monitored at 670 nm (solid line) and at 640 nm (dotted line).

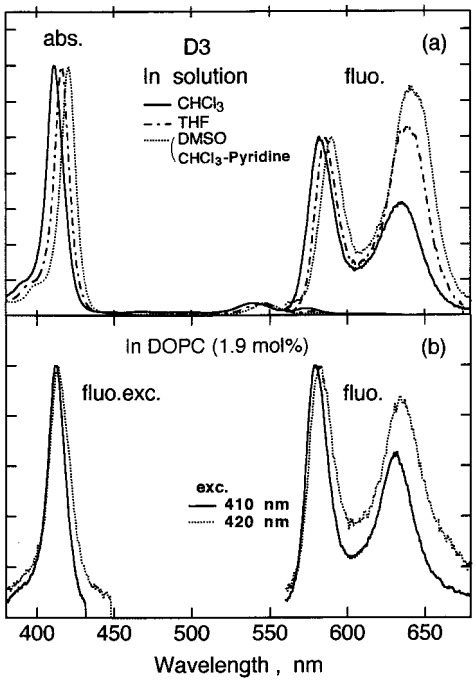

Figure 4. Absorption and steady-state fluorescence spectra of D3 in solution (a) and in LB monolayer film (b). The spectrum in $CHCl_3$−pyridine solution was the same as that in DMSO. The absorption spectra of LB films are shown in the fluorescence excitation spectra monitored at 630 nm (solid line) and at 640 nm (dotted line).

multilayered film more than single layer was not stable on a quartz substrate. Probably high fluidity and disordered arrangement of DOPC membrane make it difficult to stack multilayers. The samples of LB films used in this study, therefore, are single monolayer films.

3.2. Absorption and Fluorescence Spectra. The absorption and fluorescence spectra of D1 and D3 are shown respectively in Figures 3 and 4 for solutions and DOPC-LB films. The absorption spectra are typical of zinc porphyrin exhibiting a strong Soret band at 420 nm and a weak Q-band at 550 nm,[19] indicating no significant interaction between ZnP and Pm groups. On the other hand, the fluorescence spectra of D1 and D3 are significantly different from one another with respect to the intensity ratio between the first and second vibrational bands, $I_F(0,1)/I_F(0,0)$. In $CHCl_3$ solution as an example, I_F (0,1)/I_F (0,0) is 2.3 in D1, whereas it is 0.6 in D3. This difference indicates a significant difference among porphyrin ring structures of D1 and D3 without and with alkyl chains, respectively. Also the spectral profile depends on solvent and environmental factor; i.e., in a pure solvent of DMSO and in a mixture of $CHCl_3$ and pyridine, the value of I_F (0,1)/I_F (0,0) is 1.1 in D1, and 1.3−1.4 in D3. It may suggest that pyridine coordinates on a zinc atom of ZnP to give a spectrum identical to the spectrum in polar solvent like DMSO.

In DOPC-LB films, the absorption and fluorescence spectra of D1 (Figure 3b) are similar to the spectra in polar solvent, while the spectra of D3 (Figure 4b) are similar to those in nonpolar solvent; i.e., I_F (0,1)/I_F (0,0) is 1.13 in D1, and 0.89 in D3. This striking difference between D1 and D3 may occur from the difference in the interaction of zinc atom of ZnP with a zwitter ionic headgroup of DOPC. The anionic group of DOPC can interact with the zinc atom of ZnP, and the residual cationic group of DOPC binds to the anionic quartz surface.[13] D1 without alkyl chain in ZnP brings the polar group of DOPC near to zinc atom, resulting in a spectrum corresponding to that in polar solvent. On the other hand, D3 with alkyl chains in ZnP keeps the anionic group apart from ZnP resulting in a spectrum identical to that in nonpolar solution.

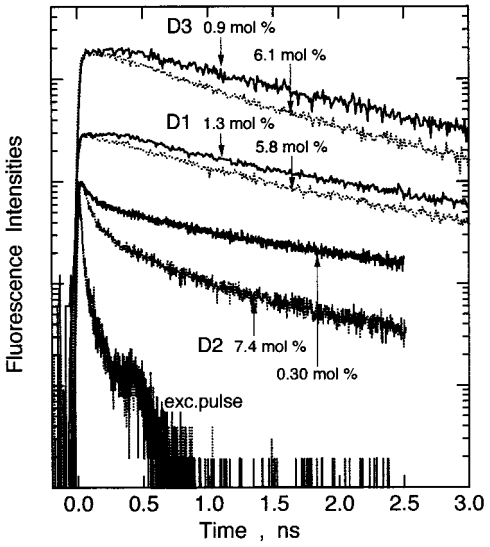

Figure 5. Fluorescence decay curves of DOPC-LB monolayer films of D1, D2 and D3 at high and low concentrations.

In consequence from the absorption and the steady-state fluorescence spectra at lower concentration, the guest molecules of D1 and D3 are distributed mostly as monomers in LB films, and the residual minor species which is responsible for an excitation-wavelength dependence on the fluorescence spectrum must be in different sites having structural conformations and/or microenvironments of slightly different energies.

3.3. Fluorescence Decays and Time-Resolved Fluorescence Spectra. Figure 5 shows fluorescence decay curves of D1, D2, and D3 in LB films with different concentrations. It is seen that the decay curves of D2 include fast and slow decaying components, whereas those of D1 and D3 consist of only slower decaying components. The fluorescence of D4 in LB monolayer

TABLE 1: Fluorescence Lifetimes and Amplitudes for D1−D4 in Solution, LB Film, and PS Polymer Film Observed at 590−600 nm

	samples	concn (mol %)	excitn wavelength (nm)	solid films τ_F (ps)	solid films A	solution[a] τ_F (ps)
D1	DOPC	1.3	412	500	0.51	180
				2300	0.49	
		5.8	412	390	0.60	
				1900	0.40	
D2	DOPC−INS	0.3	420	48	0.64	18
				436	0.17	
				2500	0.19	
		7.4	420	41	0.80	
				377	0.14	
				2000	0.07	
D3	DOPC	0.9	410	1450	1.0	27
		6.1	410	383	0.48	
				1378	0.52	
D4	Polystyrene	<0.5	415	16	0.96	13
				146	0.01	
				1788	0.03	

[a] Data from refs 3, 11, and 12.

films is very weak, and this makes it difficult to obtain reliable data of the decay curve and the lifetime value. Instead of LB films, therefore, we employed a polystyrene (PS) film for D4 which allowed us to prepare a substantially thick film and to measure the fluorescence decay curve with sufficient precision. The fluorescence lifetimes are summarized in Table 1.

In D1-LB films, the decay curve consists of two components with lifetimes of 500 ps and 2.3 ns in 1.3 mol %, and 390 ps and 1.9 ns in 5.8 mol %. The amplitude of the fast component is larger in higher concentration. In alkyl-substituted D3-LB films, similar behaviors are seen in higher concentration (6.1 mol %), but in low concentration (0.9 mol %) it gives a single-exponential decay with lifetime of 1.45 ns. The lifetime value of 1.45 ns is identical to the lifetime of ZnP monomer in LB films, suggesting that no electron transfer occurs in D3-LB film. On the other hand, D2 in INS-DOPC exhibits fast decays with lifetimes of 48 ps in 0.3 mol % and 41 ps in 7.4 mol %, as well as long decays of 400 ps to 2 ns. The fast lifetimes of 41 and 48 ps are similar to those obtained in solutions (18 ps in D2, 27 ps in D3, and 13 ps in D4) which have already been established to be due to the electron transfers.[11,12] From this viewpoint, these fast decays could be considered as due to an electron transfer, but we should pay attention to this assignment as is discussed in the next discussion. For D4 in polystyrene film, a very fast and single-exponential decay ($\tau_F = 16$ ps) was observed at room temperature and at 77 K. Since this decay time is in close agreement with that in solution, it can be interpreted as arising from the *intra*molecular electron transfer.

The time-resolved fluorescence spectra are shown in Figure 6 for D2 in INS-DOPC LB film. It is seen that the spectrum changes with time from the short time region 0−50 ps to longer time region after 50 ps. A similar spectral change is observed in higher concentration (7.4 mol %). Note that D2 without alkyl chains has a tendency to form dimers in LB films and that the later-time spectrum coincides with the steady-state fluorescence spectrum. Also noteworthy is that the time scale of spectral change (∼50 ps) corresponds to the fast decay lifetime. We assign the earlier-time spectrum as due to a dimer of D2 involved in LB films, and the later-time spectrum to D2 monomer. Therefore, the fast decays of D2 (41−48 ps) are considered to be due to an intermolecular electron transfer occurring at dimer sites from ZnP of the photoexcited molecule to Nm of the neighboring molecule. The structure of the dimer and orientation in LB film will be presented in section 3.5.

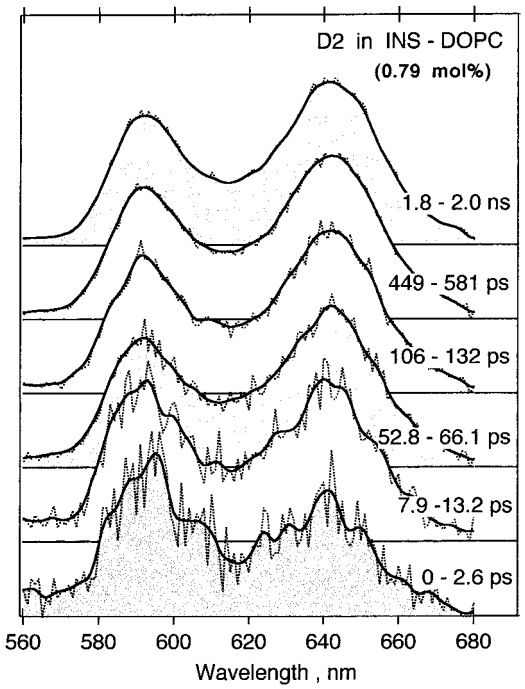

Figure 6. Time-resolved fluorescence spectra of D2-LB film of DOPC−INS mixed matrix. Excitation wavelength is 420 nm.

For the decay curves of D1 and D3 in LB films, the components of 400−500 ps lifetimes cannot be regarded as due to the electron transfer. Their nonexponential fluorescence decays should be considered to be site-dependent behaviors which can be easily met in disordered condensed matter like LB films.[20,21] It is worth noting that D1 and D3 in solution undergo fast intramolecular electron transfer (Table 1), indicating a significant role of the solvent reorganization effect.[3,11,12]

In consequence, we consider that, in LB films and/or PS films, the electron transfer occurs in D2 (intermolecular) and D4 (intramolecular), while in D1 and D3 it does not occur. It is interesting that the case of D3 exhibits a marked contrast between the LB film and the solution; a fast reaction occurs in solution whereas it does not occurs in LB films.

3.4. Free Energy for Electron Transfer. Let us consider the free energy of photoinduced electron transfer in the molecular systems of D1−D4. According to the Marcus theory,[22,23a] the electron transfer rate k_{ET} for a nonadiabatic reaction can be expressed by

$$k_{ET} = \frac{2\pi}{\hbar} \frac{H_{el}^{\ 2}}{(4\pi\lambda k_B T)^{1/2}} \exp\left[-\frac{\Delta G^*}{k_B T}\right] \qquad (1)$$

where H_{el} is the electronic coupling matrix element; k_B is the Boltzmann constant; λ ($=\lambda_i + \lambda_0$) is the reorganization energy including components from an inner-sphere term λ_i involving vibrational energy changes between the initial and final states and an outer-sphere term λ_0 involving the solvent orientation and polarization; and ΔG^* is the activation energy which can be expressed in the following equation.

$$\Delta G^* = (\Delta G^\circ + \lambda)^2/4\lambda \qquad (2)$$

where ΔG° is the standard free energy of electron transfer. The exothermicity of the reaction $-\Delta G^\circ$ is written as

$$-\Delta G^\circ = E_{S1} - (E_D^{ox} - E_A^{red} - \Delta G_S) \qquad (3)$$

where E_{S1} is the energy of the lowest singlet excited state; E_D^{ox} and E_A^{red} are respectively the half-wave potentials of one-electron oxidation of ZnP and reduction of imides which can be measured by a cyclic voltammetry; and ΔG_s is the solvent free energy change. The solvent free energy change ΔG_s is a quantity of the Coulomb energy change upon ion-pair formation and is usually expressed in the following equation by applying the Born equation.[22,23]

$$\Delta G_s = \frac{e^2}{2}\left(\frac{1}{a_D} + \frac{1}{a_A}\right)\left(\frac{1}{\epsilon_s} - \frac{1}{\epsilon_r}\right) - \frac{e^2}{\epsilon_s r_{DA}} \qquad (4)$$

where a_D and a_A are the radii of spheres of D and A, ϵ_s and ϵ_r are dielectric constants of the solvent in which the electrochemical potentials were measured and the medium in which the reaction kinetics were measured, respectively, and r_{DA} is the distance between the centers of spheres of D and A. The first term includes the difference in free energy of ion solvation between the solvent of ϵ_s and the medium of ϵ_r.

The redox potentials of donor (ZnP and ZnP′) and acceptor (Pm and Nm) groups were measured by means of a cyclic voltammetry for dimethylformamide solution. The results are $E_D^{ox} = 0.43$ V for ZnP and 0.19 V for alkyl-substituted ZnP′, and $E_A^{red} = -1.24$ V for Pm and -0.99 V for Nm. Then the $-\Delta G°$ values in $CHCl_3$ are obtained as 0.10, 0.33, 0.33, and 0.59 eV for D1−D4, respectively, from eqs 3 and 4 by using the values of $a_D = 5$ Å, $a_A = 3.5$ Å, and $r_{DA} = 11.8$ Å. A relationship of the electron transfer rate vs $-\Delta G°$ in $CHCl_3$ solution shows that the reaction rates of D1−D4 are in the normal region and particularly that of D4 lies closely at the top region of $-\Delta G°$ dependence. In DOPC-LB film, we cannot derive the $-\Delta G°$ values for D1−D4, because of lack of data for the dielectric constant and refractive index of DOPC. Then further consideration is made for polystyrene (PS) films for which these constants are known to be $\epsilon = 2.54$ and $n = 1.591$.[24] The $-\Delta G°$ values in PS films are calculated to be -0.32, -0.07, 0.01, and 0.17 eV for D1−D4, respectively. This means that the reaction can occur only in D4, and it is in accord with the experimental results. With D4, furthermore the activation energy ΔG^* (eq 2) was estimated to be 0.0013 eV in PS film and 0.016 eV in $CHCl_3$[25b] by using the literature value of $\lambda_i = 0.20$ eV.[25a] This means that the almost barrierless intramolecular electron transfer can occur in D4 both in solid film and in solution and that its rate must be irrespective of the medium and temperature. The actual experimental result shows that the fluorescence lifetime (16 ps) of D4 in PS film is not changed on lowering temperature down to 77 K. This may be accounted for, from the above estimation, by a very low activation barrier due to a small difference between the free energy change of reaction and reorganization energy of medium.

On the other hand, the fast fluorescence decay (41−48 ps) observed in D2 in INS-DOPC LB film can be considered as due to the intermolecular electron transfer at a dimer where the donor and the acceptor locate closely within DOPC matrix. Such a specific arrangement may probably result in a substantial increase in the electronic coupling H_{el} and the free energy change $-\Delta G°$. The dimer formation must be related closely to the molecular orientation in LB monolayer films, and its conformation is discussed in the next section.

3.5. Polarized Absorption Spectra of D2 in INS-DOPC LB Films. Figure 7 shows the absorption spectra around the Soret band of D2 in INS-DOPC LB films which were prepared by deposition at different surface pressures and concentrations. It is found that the spectrum depends largely on dipping pressure

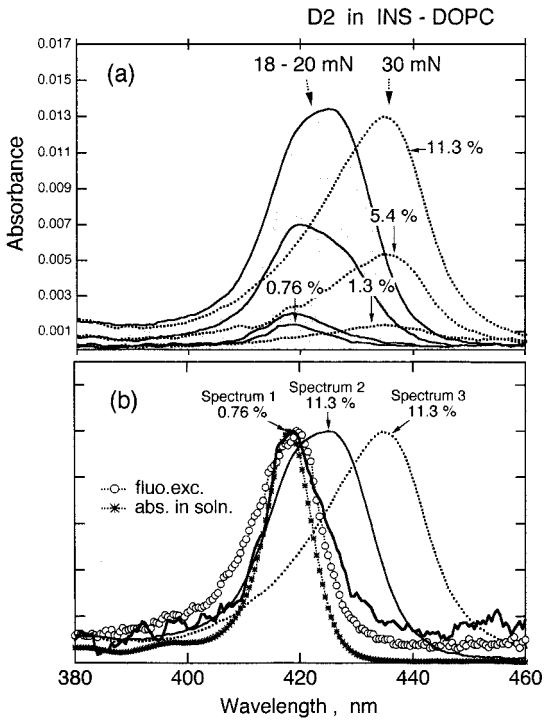

Figure 7. Absorption spectra of D2-LB film in INS-DOPC mixed matrix deposited at surface pressures of 18−20 mN and 30 mN (a), and their normalized spectra including a spectrum in solution and a fluorescence excitation spectrum (b).

even at lower concentration, and from the normalized spectra (Figure 7b) three kinds of absorption species are distinguishable; spectrum 1, centered at 419 nm which appears in 0.76 mol % at 18−20 mN deposition pressure; spectrum 2, centered at 425 nm which appears in 11.3 mol %; and spectrum 3, centered at 434 nm which appears at 30 mN deposition pressure. By comparing spectrum 1 with the spectrum of solution (Figure 7b), spectrum 1 can reasonably be assigned as due to the D2 monomer. Spectra 2 and 3 can be assigned as due to a dimer and a higher aggregate, respectively, from the concentration dependence; i.e., the spectrum is changed with increasing concentration from spectrum 1 to spectrum 3. At higher surface pressure 30 mN, D2 molecules are squeezed out from DOPC membrane resulting in a formation of higher aggregates. In contrast to the absorption spectra, the fluorescence excitation spectra (Figure 7b) are essentially the same as the monomer absorption spectrum even in higher concentration, indicating that the dimer and higher aggregates are nonfluorescent.

Since we have seen that the dimer formation correlates also with appearance of the fast fluorescence decays (41−48 ps, see Table 1), it may reasonably considered that the electron transfer in D2-LB films occurs as an *inter*molecular reaction from a donor in one molecule to an acceptor in the other molecule of the dimer.

In order to examine the molecular orientation of D2 in INS-DOPC LB film, the polarized absorption spectrum was measured in a method described in our previous paper.[26] We define the substrate-fixed Cartesian coordinates (X,Y,Z) with the origin at the center of the film. The spatial coordinates in relation to the LB film and the incident polarized light are shown in Figure 8. The X axis of the substrate is the same as the dipping direction of LB film, and the substrate is rotated about the X axis. The angle between the incident light beam and Z axis is defined as α. The polarization angle of the absorbed light, β, is defined such that $\beta = 90°$ when the polarization direction coincides with the direction of X axis. Let the transition dipole

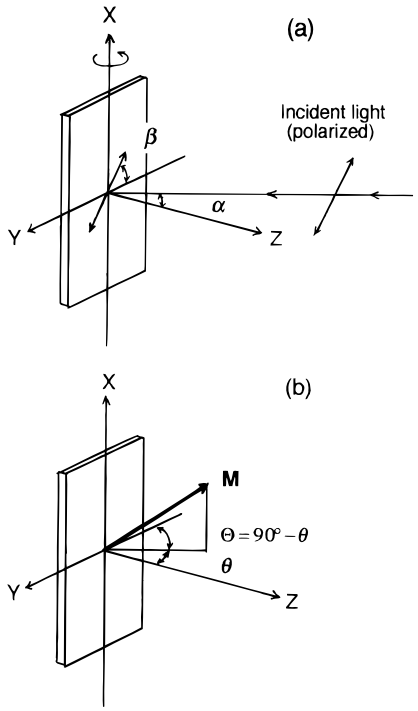

Figure 8. Spatial coordinates for the sample and the optical geometry: (a) the direction of polarized incident light and the rotation of the sample, and (b) the direction of the transition dipole moment of ZnP in a monolayer film.

moment vector **M** of ZnP be oriented at an angle θ to the *Z*-axis, then Θ defined as $\Theta = 90°-\theta$ gives a tilt angle of **M** to the substrate plane (*XY* plane). When a polarized light with polarization angle β is illuminated on the film at incident angle α and the refraction angle α' in an air−monolayer interface, the absorption intensity $A(\alpha',\beta)$ and the dichroic ratio *R* can be given in eqs 5 and 6, respectively.

$$A(\alpha',\beta) \propto \sin^2\theta + (3\cos^2\theta - 1)\sin^2\alpha'\sin^2\beta \qquad (5)$$

$$R = \frac{A(\alpha',90)}{A(\alpha',0)} = \cos^2\alpha' + 2\cot^2\theta\sin^2\alpha' \qquad (6)$$

where

$$A(\alpha',0) = A_{obs}(\alpha',0)\cos\alpha' \propto \sin^2\theta = \text{const} \qquad (7)$$

The θ or Θ values can be obtained by measuring the absorption intensity (eq 5) and/or the dichroic ratio (eq 6) as functions of the polarization angle β and the refraction angle α' (or incident angle α). The refraction angle α' was evaluated from eq 7 as a correction factor ($\cos\alpha'$) in an optical path length.

First, we examined, for the two types of INS-DOPC LB films of D2 deposited at 18 and 30 mN, the absorption intensity change by varying the polarization angle β of the incident light under irradiation along *Z* axis, i.e., $\alpha' = 0$. As a result, the absorption intensities at wavelengths covering monomer, dimer, and higher aggregates were constant irrespective of β. By taking eq 5 into consideration, it follows that all the species of D2 are distributed randomly around *Z* axis with respective values of tilt angle θ. Next, in order to estimate θ values from the dichroic ratio (eq 6), we measured the absorption spectra with $\beta = 0°$ and 90° at $\alpha = 30°$ and 45°. The results are shown in Figure 9a,b (normalized spectra). It is seen in the normalized spectra that the spectral profiles are different depending on α and β around 420 nm corresponding to spectrum 1, indicating that

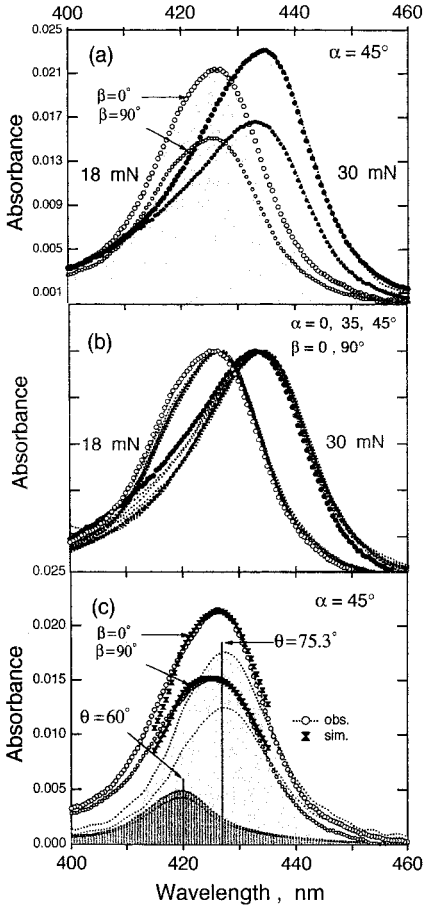

Figure 9. Polarized absorption spectra of D2-LB film in INS-DOPC mixed matrix with concentration of 12 mol %: (a) the incident angle $\alpha = 45°$ with the polarization angle $\beta = 0°$(s-polarized) and 90° (p-polarized), (b) normalized spectra at $\alpha = 0°$, 30°, and 45° with $\beta = 0°$ and $\beta = 90°$, and (c) analyzed component spectra for monomer and dimer at $\alpha = 45°$ with $\beta = 0°$ and $\beta = 90°$. These spectra were used for calculation of the dichroic ratio.

spectrum 1 has a θ value different from the dimer and higher aggregate. In the foregoing discussion on concentration dependence of the isotropic spectra shown in Figure 7a,b, we assign spectrum 1 as due to monomer. Then each of the two spectra at $\beta = 0°$ and 90° was analyzed into components of monomer and dimer by curve fitting with θ as a parameter, assuming the band profile of the monomer as shown in Figure 7b. From the best fit curves, the dichroic ratios were measured, and finally the θ values were estimated from eq 6 to be $\theta = 60°$ for monomer, and $\theta = 75.3°$ for dimer. For higher aggregates, the intensity at 440 nm was directly analyzed because of the contribution of monomer negligibly small in this wavelength, and finally the θ values were evaluated to be 60°, 75.3°, and 80° for monomer, dimer, and higher aggregates, respectively. To confirm the validity of these values, the absorption intensities were measured as functions of α and β and compared the resultant curves with the curves calculated from eq 5. The results are shown in Figure 10. It is seen that the experimental curves are fitted well to the calculated curves of $\theta = 75°$ for the dimer band and of $\theta = 80°$ for the higher aggregate band, indicating that evaluated θ values are reasonable. The θ value obtained at monomer band ($\theta = 60°$) is close to the magic angle, and it corresponds to the experimental result that the absorption intensity is constant irrespective of α and β.

Finally, we focus discussion on the conformation of dimer in INS-DOPC LB monolayer film based on the absorption

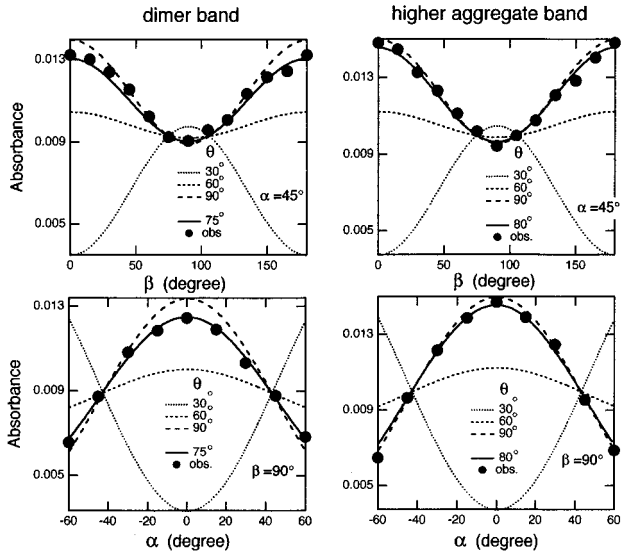

Figure 10. Plots of absorbance (solid circles) as functions of α and β at 432 nm for dimer and at 440 nm for higher aggregates. Broken lines show absorbance change by varying values of α and β, and solid lines are best fitted to the experimental plots.

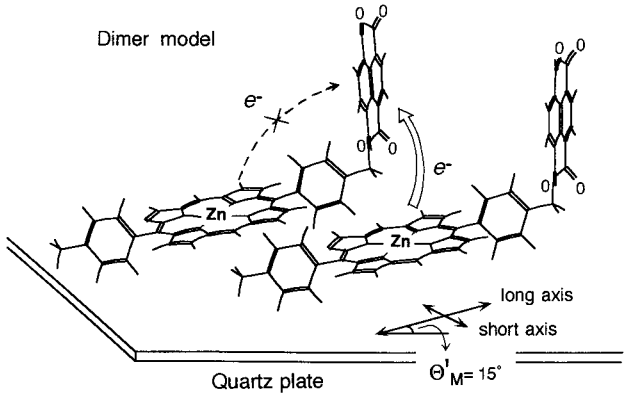

Figure 11. Spatial orientation and arrangement of D2 dimer in a DOPC-INS LB monolayer film. The tilt angles of long and short axes of ZnP to a substrate plane are 15°. This model illustrates an intermolecular electron transfer from ZnP to Nm between neighboring D2 molecules.

profile of the Soret band. It is known that, in the monomer of zinc porphyrin, the excited singlet states for the Soret band are doubly degenerate with their transition dipole moments being at right angles, i.e., long axis and short axis (see Figure 11). For the present case of dyads D1−D4, the Soret band of ZnP is considered to be still degenerate and involves the doubly degenerate transitions. For the ZnP dimer, the exciton splitting of Soret band is known to give two allowed transitions even in a coplanar head-to-tail linear conformation because of the degenerate monomer states.[29,30] The energy levels and absorption intensity ratio of two exciton bands depend on the distance and angle between the transition dipole moments of the component monomer $\mathbf{M}_m'$. It has been shown by Osuka et al.[29,30] that, in a series of naphthalene-bridged dimeric porphyrins, most of diporphyrins give a larger absorption intensity at lower energy band and the higher energy band lies coincidentally very close to the monomer band. Therefore, the dimer band at 427 nm in LB film showing no apparent splitting contains two exciton bands having the same θ or Θ value. By taking into consideration the band shape similar to that of 1,5- or 1,4-naphthalene bridged diporphyrin,[30] it is considered that two ZnP's in the dimer take not an oblique but slightly slipped head-to-tail configuration with parallel plane each other.

It is found in the foregoing discussion that the monomer distributes randomly or isotropically inside a monolayer with a tilt angle $\Theta_m = 30°$ to the substrate surface. Since the direction of transition dipole moment of the dimer $\mathbf{M}_d$ is given by a sum of two transition moment vectors of the component monomer $\mathbf{M}_m'$, the tilt angle of dimer Θ_d must lie between the tilt angle of the component monomer Θ_m' and 90°, depending on the angle between two transition moments $\mathbf{M}_m$'s. Assuming that the dimer takes a slipped head-to-tail conformation with two ZnP planes being in parallel as described above, two $\mathbf{M}_m$'s are in parallel, i.e., $\Theta_d = \Theta_m'$. Note that the observed value of Θ_d is 15°, then we obtain $\Theta_m' = 15°$, indicating that the component ZnP becomes more parallel to the substrate surface than the free monomer. Thus the possible spatial orientation and arrangement of dimers in the LB monolayer is illustrated in Figure 11.

In the dimer obtained at lower dipping pressure, where the two ZnP's are partially overlapped, the distance between ZnP and the neighboring Nm is fairly short and the angle between the planes of two groups is as small as 70°. Such close location and orientation between donor and acceptor may result in substantial increases in the electronic coupling between reactant and product and Coulombic interaction in an ion-pair state leading to a fast intermolecular electron transfer in the dimer. The higher aggregate, which forms at higher dipping pressure where ZnP dyads are squeezed out from a monolayer, may possibly take a similar head-to-tail slipped conformation and the fast intermolecular electron transfer can take place similarly to the case of inner layer dimer.

4. Concluding Remarks

The intramolecular electron transfer has been studied with different types of ZnP−imide dyads incorporated into a LB film of unsaturated phospholipid DOPC matrix. Care has to be taken to satisfy the condition of monomer dispersion of macromolecules in monolayer films: (1) chemical modification by addition of alkyl groups peripherally to porphyrin ring (D3 and D4), (2) mixed matrix of INS and DOPC, and (3) dipping pressures lower and higher than the phase transition pressure, in higher pressure of which dimers and/or higher aggregates are major species. The time-resolved fluorescence measurement has revealed that the *intra*molecular electron transfer in LB films occur in D4, but not in D1, D2, and D3. This is in striking contrast to the cases of solution ($CHCl_3$) where the *intra*molecular electron transfer takes place. These reaction characteristics are discussed in terms of the free energy $-\Delta G°$ for the intramolecular electron transfer reaction on the basis of a conventional electron transfer theory. The theoretical treatments are approximately in accord with the experimental results, indicating that, although an interaction between ZnP and the anionic headgroup of DOPC is significant from the absorption and fluorescence spectra of dyads, the stabilization of ZnP^+ by DOPC is not enough to compensate the reduced reaction exergonicity in solid state. In the case of D4, it is found that a fast intramolecular transfer rate is irrespective of medium and temperature. This is interpreted well in terms of a low activation barrier in the reaction with small difference between the free energy change and reorganization energy.

In the case of D2-LB films, despite efforts to prepare the LB film of monomer dispersion, nonfluorescent dimer and higher aggregates are formed at the inner and outer layer of the membrane in the INS-DOPC matrix even at lower concentra-

tions. The fluorescence quenching can be interpreted as due to the intermolecular electron transfer at dimer sites, from ZnP of one molecule to Pm or Nm of the other molecule of the dimer. From analyses of the polarized absorption spectra, a dimer conformation of a slightly slipped head-to-tail structure of ZnP is obtained. Under such an arrangement, a partial overlap between donor and acceptor is possible leading to the fast fluorescence quenching by intermolecular electron transfer.

References and Notes

(1) Barbara, P. F.; Meyer, T. J.; Ratner, M. A. *J. Chem. Phys*. **1996**, *100*, 13148.

(2) Wasielewski, M. R. *Chem. Rev*. **1992**, *92*, 435.

(3) Osuka, A.; Marumo, S.; Mataga, N.; Taniguchi, S.; Okada, T.; Yamazaki, I.; Nishimura, Y.; Ohno, T.; Nozaki, K. *J. Am. Chem. Soc*. **1996**, *118*, 155.

(4) Gust, D.; Moore, T. A.; Moore, A. L. *Acc. Chem. Res*. **1993**, *26*, 198.

(5) Harriman, A.; Heitz, V.; Ebersole, M.; van Willigen, H. *J. Phys. Chem*. **1994**, *98*, 4982.

(6) Pollinger, F.; Heitele, H.; Michel-Beyerle, M. E.; Anders, C.; Futscher, M.; Staab, H. A. *Chem. Phys. Lett.* **1992**, *198*, 645.

(7) Fleming, G. R.; Van Grondelle, R. *Phys. Today* **1994**, *47*, 48.

(8) Hu, X.; Schulten, K. *Phys. Today* **1997**, *50*, 28. Tavan, P.; Schulten, K. *Phys. Rev. B* **1987**, *36*, 4337.

(9) Jonas, D. M.; Fleming, G. R. *J. Phys. Chem*. **1996**, *100*, 12660.

(10) Stanley, R. J.; Boxer, S. G. *J. Phys. Chem*. **1996**, *100*, 12052.

(11) Osuka, A.; Nakajima, S.; Maruyama, K.; Mataga, N.; Asahi, T.; Yamazaki, I.; Nishimura, Y.; Ohno, T.; Nozaki, K. *J. Am. Chem. Soc*. **1993**, *115*, 4577.

(12) Osuka, A.; Marumo, S.; Maruyama, K.; Mataga, N.; Tanaka, Y.; Taniguchi, S.; Okada, T.; Yamazaki, I.; Nishimura, Y. *Bull. Chem. Soc. Jpn*. **1995**, *68*, 262.

(13) Petrov, J. G.; Möbius, D. *Langmuir* **1991**, *7*, 1495.

(14) Dick, H. A.; Bolton, J. R.; Picard, G.; Munger, G.; Leblanc, R. M. *Langmuir* **1988**, *4*, 133.

(15) Gust, D.; Moore, T. A.; Moore, A. L.; Luttrull, D. K.; DeGraziano, J. M.; Boldt, N. J.; Van der Auweraer, M.; De Schryver, F. C. *Langmuir* **1991**, *7*, 1483.

(16) Vuorima, E.; Ikonen, M.; Lemmetyinen, H. *Chem. Phys*. **1994**, *188*, 289.

(17) Fu, Y.; Jayaraj, K.; Lever, A. B. P. *Langmuir* **1994**, *10*, 3836.

(18) Tamai, N.; Matsuo, H.; Yamazaki, T.; Yamazaki, I. *J. Phys. Chem.* **1992**, *96*, 6550.

(19) Gouterman, M. In *The Porphyrins Vol. III, Physical Chemistry, Part A*; Dolphin, D., Ed.; Academic Press: New York, 1978; Chapter 1, pp 1−165.

(20) Yamazaki, I.; Tamai, N.; Yamazaki, T. *J. Phys. Chem*. **1990**, *94*, 516.

(21) Tamai, N.; Yamazaki, T.; Yamazaki, I. *Can. J. Phys.* **1990**, *68*, 1013.

(22) Siders, P.; Marcus, R. A. *J. Am. Chem. Soc*. **1981**, *103*, 748.

(23) (a) Marcus, R. A.; Sutin, N. *Biochim. Biophys. Acta* **1985**, *811*, 265. (b) Marcus, R. A. *J. Chem. Phys*. **1956**, *24*, 966.

(24) Altmann, R. B.; Renge, I.; Kador, L.; Haarer, D. *J. Chem. Phys*. **1992**, *97*, 5316.

(25) (a) Liu, J.; Bolton, J. R. *J. Phys. Chem*. **1992**, *96*, 1718. (b) λ_0 was calculated from the Marcus expression[23b]

$$\lambda_0 = (\Delta e)^2\left[\frac{1}{2a_D} + \frac{1}{2a_A} - \frac{1}{r_{DA}}\right]\left[\frac{1}{\epsilon_D} - \frac{1}{\epsilon_s}\right]$$

where ϵ_{op} and ϵ_s are the optical and static dielectric constatnts of the surrounding medium.

(26) Ohta, N.; Matsunami, S.; Okazaki, S.; Yamazaki, I. *Langmuir* **1994**, *10*, 3909.

(27) Nakamura, H.; Terazima, M.; Hirota, N.; Nakajima, S.; Osuka, A. *Bull. Chem. Soc. Jpn*. **1995**, *68*, 2193.

(28) Eriksson, S.; Källebring, B.; Larsson, S.; Mårtensson, J.; Wennerström, O. *Chem. Phys*. **1990**, *146*, 165.

(29) Osuka, A.; Maruyama, K. *J. Am. Chem. Soc*. **1988**, *110*, 4454.

(30) Nagata, T.; Osuka, A.; Maruyama, K. *J. Am. Chem. Soc.* **1990**, *112*, 3054.